



First Photometric Investigation of the Neglected EW-type Binary System V502 Her

Zhao Ergang^{1,2,3,4}, Qian Shengbang^{1,2,3,4}, Liao Wenping^{1,2,3}, He Jiajia^{1,2,3}, Shi Xiangdong^{1,2,3}, and Zhang Jia^{1,2,3}

¹ Yunnan Observatories, Chinese Academy of Sciences (CAS), P.O. Box 110, 650216 Kunming, People's Republic of China; zergang@ynao.ac.cn

² Key Laboratory for the Structure and Evolution of Celestial Objects, Chinese Academy of Sciences, 650216 Kunming, People's Republic of China

³ Center for Astronomical Mega-Science, Chinese Academy of Sciences, 20A Datun Road, Chaoyang District, Beijing, 100012, People's Republic of China

⁴ University of the Chinese Academy of Sciences, Yuquan Road 19#, Shijingshan Block, 100049 Beijing, People's Republic of China

Received 2017 October 15; accepted 2018 January 17; published 2018 March 12

Abstract

V502 Her is a neglected EW-type binary, which has been known for more than 60 years. The first multi-color CCD photometric light curve and spectroscopic observations of contact binary V502 Her was obtained. Based on the LAMOST data, its spectrum can be found to be F5. Together with solutions of light curves by using the Wilson-Devinney code, it infers that V502 Her is an A-type W UMa contact binary system with the mass ratio of $q = 0.313$ and the filling factor of $f = 38.1\%$. According to all minimum times from the literature and our observations, the orbital period was analyzed and a long-term increase with a periodic change ($P_3 = 26.8$ years) was computed. The orbital period increase may be caused by the mass transfer from a less-massive component to the more massive one, which indicates that V502 Her is in the thermal relaxation oscillation (TRO) controller stage, while the light-travel time effect (LTTE) through the presence of a cool third body may lead to the periodic variation.

Key words: (stars:) binaries: eclipsing – (stars:) binaries: spectroscopic – (stars:) binaries (including multiple): close

Online material: color figures

1. Introduction

V502 Her (also named GSC 02610-02223, NSVS 8045257) was discovered as a variable star by Hoffmeister (1949), then Gessner (1966) determined its period as 0.3117 days. More than 10 years later, Hoffmann & Meinunger (1983) obtained the corrected light elements and found no period change between JD 2430938.493 and 2445140.50 by using the photoelectric photometry in 1982 and other minimum times. In the fourth edition of the General Catalogue of Variable Stars (GCVS), V502 Her was classified as an EW/KW-type binary and its magnitude was about 12.8–13.7. For dozens of years, many light minimums had been given in visual, photoelectric and CCD by several authors, such as Safar & Zejda (2000a, 2000b, 2002c), Agerer & Hubscher (2003), Hubscher et al. (2012), and others, but so far there was no detailed photometric investigations have been published. Therefore, we listed V502 Her into the monitoring pool of contact binary observation program.

In this paper, we present complete B , V , R and I light curves of V502 Her. By using the Wilson-Devinney code, photometric solutions of this binary were obtained for the first time. Orbital period investigations occupy an important position in close binary studies. It can imply information about physical processes occurring in binaries, such as mass transfer (Qian 2001), magnetic activity cycles (Applegate &

Patterson 1987), and interaction with a tertiary body (Irwin 1952). Therefore, we analyze the long-term orbital period variation of V502 Her based on all available times of light minimum.

2. New Photometric and Spectroscopic Observations

To analyze the light curve and period variation, V502 Her has been observed several times from 2007 to 2013 by three telescopes: the 1-meter telescope at Yunnan observatories (YNOs 1m), the 60-centimeter telescope at Yunnan observatories (YNOs 60 cm), and the 85-centimeter telescope at Xinglong station of National Astronomical Observatories (Xinglong 85 cm) in China. The camera attached on Cassegrain focus of YNOs-1 m is DW436 CCD from Andor Technology, whose field is about 7.5×7.5 arcmin². The YNOs 60 cm used the same camera as YNOs 1 m, but has a large field of view, about 12.5×12.5 arcmin². The first B , V , R , and I light curves were obtained during three nights in 2011, with the PI 512 \times 512 TE CCD camera mounted on the Xinglong 85-cm telescope. The effective field of view of the photometric system is 14.5×14.5 arcmin² at prime focus. The color systems were close to the standard Johnson-Cousin-Bessel $UBVRI$ CCD photometric system (Zhou et al. 2009). The integration times for each image were 50 s in the B band, 30 s in the V band, 20 s in the R band, and 10 s in the I band. For each band, about 200

Table 1
Coordinates of V502 Her, the Comparison and the Check Stars

Targets	α_{2000}	δ_{2000}
V502 Her	$17^{\text{h}}35^{\text{m}}49^{\text{s}}.3$	$+32^{\circ}20'54''.5$
The comparison	$17^{\text{h}}35^{\text{m}}38^{\text{s}}.8$	$+32^{\circ}18'02''.1$
The check	$17^{\text{h}}36^{\text{m}}21^{\text{s}}.9$	$+32^{\circ}20'32''.1$

images were obtained, 203 images in *B*, 203 images in *V*, 202 images in *R*, and 201 images in *I*. The Image Reduction and Analysis Facility (IRAF) was used to reduce these hundreds of images. Differential photometry was used for these images and the coordinates of V502 Her; the comparison and check stars are listed in Table 1. The observed light curves are plotted in Figure 1, which are calculated by the ephemeris shown in the figure. The new determined times of light minimum from these three telescopes are computed and listed in Table 2, where filter N means no filter.

From light curves in Figure 1, it is obvious that depths of eclipse are different in bands. By calculating the difference between phase 0.0 and 0.25, we found that the depth decrease with wavelength, meaning that it has large gap between maximum and minimum in the high-frequency wave, listed in Table 3.

We searched the observations of this binary in the database and found that it is one target of the Wide Angle Search for Planets (WASP). It has been observed more than 100 times from 2004 to 2008. We got the data from the WASP data release (<http://wasp.cerit-sc.cz/form>). From these data, we picked up 166 observation times and calculated minimum times, listed in Table 4, by adopting the parabolic curve to fit the minimum data in least-squares method.

From LAMOST (Large Sky Area Multi-Object Fiber Spectroscopic Telescope), we find the spectroscopic observation of V502 Her. That is the first time spectroscopic observation was given, and we obtained the data of V502 Her from LAMOST, shown in upper panel of Figure 2 and listed in Table 5. From the data, the spectrum is found to be F5. During the lower panel of Figure 2, we show the data from 3800 to 4600 Å. By contrasting it with the spectra listed in Figure 6.1 of Gray & Corbally (2009), it is very near the spectra of HR 5634 from the G-band, H δ , H γ , GaI4226, FeI4046, etc..

3. Orbital Period Investigation

After Hoffmann & Meinunger (1983) obtained no period change between JD 2430938.493 and 2445140.50, there is no period analyses for nearly 40 years. To investigate the orbital period variation of V502 Her, we collected all available times of light minimum in visual, photographic, photoelectric, and

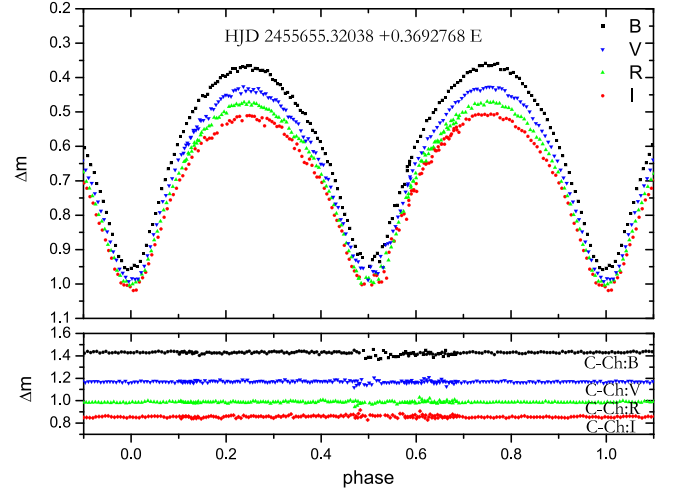


Figure 1. New light curves of V502 Her observed by the Xionglong 85 cm telescope of National Astronomical Observatories of China. Upper panel: different colored dots represent Δm between V502 Her and comparison in BVRI bands. Bottom panel: Δm between comparison and check star in BVRI bands.

(A color version of this figure is available in the online journal.)

CCD camera from the literature (listed in Table 6). Using the following ephemeris given by Hoffmann & Meinunger (1983),

$$\text{Min.}I = \text{HJD}2430938.4952 + 0.3692768 \times E, \quad (1)$$

we computed the $O - C$ values for all times of light minimum; the corresponding $O - C$ curves are drawn in the upper panel of Figure 3. A continuous period increase can be seen from the $O - C$ curve; a least-square solution yields the following quadratic ephemeris:

$$\begin{aligned} \text{Min.}I = & \text{HJD} 2430938.4980(16) + 0.36927596(11) \times E \\ & + 1.62(17) \times 10^{-11}E^2 + 3.2(9) \times 10^{-3} \\ & \times \sin[0^{\circ}.0136 \times E - 58^{\circ}.4(3^{\circ}.9)]. \end{aligned} \quad (2)$$

Based on the quadratic part of this ephemeris, a continuous period increase rate can be determined to be $dP/dt = 3.2 (\pm 0.3) \times 10^{-8} \text{ days yr}^{-1}$. The residuals from the quadratic of Equation (2) are shown in the middle panel of Figure 3. We find that there may be a periodic change of about 26.8 years by using the Photoelectric and CCD data. The residuals from Equation (2) are shown in the lower panel of Figure 3, where there is no obvious changes, suggesting that this equation fits well.

4. Light Curve Analysis Using the W-D Code

The *B*, *V*, *R*, and *I* light curves of V502 Her were simultaneously analyzed using the W-D program (Wilson & Devinney 1971; Wilson 1990, 1994, 2012). According to Lucy

Table 2
New Observe Times of Light Minimum of V502 Her

JD(Hel.)	Errors	Min.	Filters	Telescope	Date
2454890.36208	0.00023	S	<i>R</i>	YNOs 1 m	2009-02-27
2455078.13825	0.00077	P	<i>R</i>	YNOs 60 cm	2009-09-03
2455262.40906	0.00032	P	<i>R</i>	YNOs 60 cm	2010-03-06
2455302.29110	0.00038	P	<i>R</i>	YNOs 60 cm	2010-04-15
2455316.32392	0.00030	P	<i>RV</i>	YNOs 1 m	2010-04-29
2455319.27809	0.00044	P	<i>R</i>	YNOs 60 cm	2010-05-02
2455655.32028	0.00020	P	<i>BVRI</i>	Xinglong 85 cm	2011-04-03
2455665.28997	0.00059	P	<i>R</i>	YNOs 60 cm	2011-04-13
2456388.33702	0.00045	P	<i>NI</i>	YNOs 60 cm	2013-04-05

Note. Third column: P means primary minimum; S means secondary minimum. The fourth column lists the filters used to observe where *N* means no filter used.

Table 3
The Depths of Eclipse in Different Bands

Bands	Δm between Phase 0.0 and 0.25
B	0.581
V	0.551
Rc	0.533
Ic	0.517

(1967) and Ruciński (1969), and gravity-darkening coefficients of $g_1 = g_2 = 0.32$ and bolometric albedo coefficients of $A_1 = A_2 = 0.5$ were set, which are appropriate for stars having convective envelopes. Bolometric and bandpass square-root limb-darkening parameters were taken from van Hamme’s paper (1993). The following were the adjustable parameters: the orbital inclination, i ; the mean effective temperature of star 2, T_2 ; the monochromatic luminosity of star 1 in each band, L_1 and the dimensionless potential of star 1, Ω_1 .

According to the LAMOST data, the effective temperature of primary component was adopted to be $T_1 = 6180$ K (Qian et al. 2017). From Figure 1, we could find out that the new determined light curves are EW-type light curves; these two minimums are nearly symmetric and no spotted solution is needed. Extensive studies by Hoffmann & Meinunger (1983) have revealed that V502 Her is a contact binary, so the contact model (Mode 3, $\Omega_1 = \Omega_2$) is adopted in the solutions. There is no mass ratio from the spectroscopic observation, so we search the mass ratio first. We fix the mass ratio q to each value and set the other parameters free, such as i , T_2 , L_1 , Ω_1 and so on. For each q from 0.1 to 4.5 in small steps, we can get a convergence of solutions and the sum of residual ($\sum(O - C)^2$), and in total we could get the relation between q and \sum , which is shown in Figure 3. From this relation in Figure 3, we can see that the \sum has the lowest value when q is 0.3. So $q = 0.3$ is chosen as the original value, and then the mass ratio is set to be free. Finally, we get the solutions for the *B*, *V*, *R*, and *I* light curves of V502 Her, listed in Table 7. In Figure 4, we can see

the light curves are fit well, where dots in colors represent observations in different bands and lines mean the theoretical light curves.

5. Discussions and Conclusions

It has been over half of a century since V502 Her was discovered, but there was no observation given the light curves and spectrum, except some light minimums. In this paper, We presented the spectrum and *BVRI* multi-bands CCD photometric light curves for first time. From the spectroscopic data of LAMOST listed in Figure 2, there is no obvious emission, which indicates that the magnetic activity of V502 Her may be relatively weak. The smooth light curves and nearly the same magnitude in phase 0.25 and 0.75 of light curves in all bands are supporting that conclusion. From Table 5, the metallicity ($[Fe/H]$) is given as $-0.190(\pm 0.074)$, which is in agreement with Qian et al. (2017)’s Figure 5, which gives the distribution of metallicity for EW-type binaries observed by LAMOST.

We analyzed the completed light curves of V502 Her by using the WD code and obtained the photometric solutions. Based on the solutions, the mass ratio of the system (M_2/M_1) was determined to be 0.313, the orbital inclination i is 79.3 degrees, the temperature of the secondary is nearly the same as that of the primary, the contribution from the primary component to the total luminosity of system in *B*, *V*, *R*, and *I* bands is 72.7% in the *B* band, 72.9% in the *V* band, 73.0% in the *R* band, and 73.0% in the *I* band. The fill-out factor is about 38.1%. From the spectrum of LAMOST, the primary component is an F5-type main-sequence star, and the mass was estimated to be $1.23 M_\odot$ from empirical law (Gazeas 2009). Using the mass ratio, the mass of secondary can be calculated to be $0.38 M_\odot$. From structure of Figure 6, it is obvious that the system is a total eclipsing system.

From the change of the orbital period, we can see the long-term increase at a rate of $dp/dt = 3.2(\pm 0.3) \times 10^{-8}$ days yr^{-1} .

Table 4
New Calculated Times of V502 Her from SWASP Database

JD(Hel.)(Err)	JD(Hel.)(Err)	JD(Hel.)(Err)	JD(Hel.)(Err)	JD(Hel.)(Err)
2453128.5367(0.0009)	2453170.6328(0.0006)	2453200.5443(0.0006)	2453855.6395(0.0004)	2454637.5936(0.0011)
2453129.6433(0.0012)	2453171.5579(0.0005)	2453201.4688(0.0006)	2453856.5627(0.0004)	2454638.5151(0.0015)
2453130.5628(0.0015)	2453172.4793(0.0006)	2453202.5743(0.0005)	2453882.6036(0.0008)	2454639.6185(0.0014)
2453132.5958(0.0009)	2453172.6642(0.0005)	2453203.4988(0.0005)	2453883.5227(0.0005)	2454640.5453(0.0006)
2453137.5830(0.0005)	2453173.5873(0.0004)	2453204.6070(0.0004)	2453885.5546(0.0006)	2454642.5764(0.0007)
2453138.6899(0.0004)	2453174.5109(0.0004)	2453205.5283(0.0006)	2453887.5861(0.0006)	2454643.4984(0.0006)
2453139.6161(0.0005)	2453175.4364(0.0005)	2453207.5615(0.0003)	2453901.6177(0.0006)	2454644.6051(0.0006)
2453141.6456(0.0006)	2453175.6182(0.0004)	2453208.4825(0.0004)	2453902.5423(0.0007)	2454645.5317(0.0005)
2453142.5686(0.0005)	2453176.5427(0.0005)	2453209.4098(0.0006)	2453904.5758(0.0007)	2454646.4526(0.0007)
2453143.6752(0.0004)	2453177.6503(0.0005)	2453218.4521(0.0010)	2453905.4988(0.0006)	2454646.6389(0.0005)
2453144.6001(0.0005)	2453178.5719(0.0003)	2453220.4858(0.0006)	2453906.4196(0.0005)	2454647.5613(0.0006)
2453146.6331(0.0012)	2453179.4970(0.0004)	2453221.4090(0.0008)	2453906.6057(0.0003)	2454650.5152(0.0006)
2453150.6918(0.0006)	2453179.6784(0.0008)	2453223.4387(0.0006)	2453920.4545(0.0007)	2454652.5482(0.0005)
2453151.6172(0.0005)	2453180.4199(0.0006)	2453224.5471(0.0007)	2453922.4839(0.0007)	2454656.6097(0.0006)
2453152.5391(0.0004)	2453180.6037(0.0003)	2453227.5018(0.0004)	2453943.5326(0.0005)	2454657.5320(0.0005)
2453153.4640(0.0006)	2453181.5265(0.0004)	2453228.4255(0.0005)	2453944.4573(0.0003)	2454659.5616(0.0010)
2453153.6464(0.0004)	2453182.4516(0.0004)	2453229.5324(0.0004)	2453946.4871(0.0003)	2454663.4394(0.0010)
2453154.5705(0.0005)	2453182.6337(0.0005)	2453230.4558(0.0003)	2453947.4110(0.0004)	2454668.4269(0.0007)
2453155.4945(0.0008)	2453183.5579(0.0006)	2453232.4866(0.0006)	2453948.5173(0.0005)	2454669.5357(0.0014)
2453155.6752(0.0007)	2453184.4809(0.0007)	2453235.4411(0.0004)	2454191.6889(0.0013)	2454670.4586(0.0006)
2453156.5987(0.0006)	2453184.6647(0.0007)	2453237.4726(0.0003)	2454194.6478(0.0016)	2454671.5627(0.0009)
2453158.4512(0.0016)	2453185.5890(0.0006)	2453238.3951(0.0005)	2454297.4876(0.0006)	2454672.4875(0.0005)
2453158.6311(0.0008)	2453190.5740(0.0008)	2453239.5032(0.0007)	2454298.5942(0.0006)	2454673.4100(0.0004)
2453162.5094(0.0007)	2453192.4227(0.0005)	2453240.4254(0.0006)	2454305.4286(0.0009)	2454674.5165(0.0005)
2453162.6954(0.0010)	2453192.6048(0.0007)	2453242.4572(0.0007)	2454306.5336(0.0012)	2454675.4413(0.0004)
2453163.4342(0.0005)	2453194.4521(0.0006)	2453245.4099(0.0007)	2454307.4569(0.0013)	2454680.4258(0.0004)
2453163.6174(0.0006)	2453194.6365(0.0006)	2453250.3972(0.0007)	2454317.4240(0.0008)	2454681.5355(0.0008)
2453164.5395(0.0006)	2453195.5588(0.0006)	2453252.4275(0.0004)	2454322.4112(0.0007)	2454682.4570(0.0004)
2453165.6483(0.0006)	2453196.4844(0.0006)	2453254.4601(0.0011)	2454329.4294(0.0007)	2454684.4882(0.0004)
2453166.5726(0.0005)	2453197.4083(0.0009)	2453255.3815(0.0004)	2454331.4590(0.0007)	2454686.5200(0.0008)
2453167.4958(0.0005)	2453197.5897(0.0005)	2453262.3977(0.0005)	2454334.4139(0.0009)	
2453167.6778(0.0005)	2453198.5137(0.0005)	2453277.3558(0.0009)	2454585.7076(0.0007)	
2453168.6023(0.0004)	2453199.4378(0.0004)	2453851.5798(0.0007)	2454586.6298(0.0007)	
2453169.5262(0.0005)	2453199.6196(0.0006)	2453853.6115(0.0006)	2454632.6067(0.0008)	

To explain the long-term period changes of contact binary stars, Qian (2003) proposed an evolutionary scenario in which contact binaries undergo thermal relaxation oscillation (TRO; e.g., Lucy 1967; Flannery 1976; Robertson & Eggleton 1977) via a change of the contact degree. Many contact binaries, listed in Table 8, have continuous period increasing. The secular period increase of V502 Her may imply that it is on the TRO-controlled stage of this evolutionary strategy. If the continuous period increase is due to the conservative mass transfer from the secondary component to the primary, using the well-known equation

$$\frac{\dot{P}}{P} = 3\dot{M}_2 \left(\frac{1}{M_1} - \frac{1}{M_2} \right), \quad (3)$$

the mass transfer at a rate of $dM_2/dt = 1.85 \times 10^{-8} M_{\odot} \text{ yr}^{-1}$ was determined. As the mass transfer from the less-massive component to the more massive one, the contact configuration

Table 5
The Parameters Obtained from LAMOST

Observed date	2013-05-31
Exposure time	2512s
Spectral type	F5
The effective temperature(K)	6180(\pm 79)
Metallicity[Fe/H]	-0.190(\pm 0.074)
Radial velocity(km/s)	-13.54(\pm 6.62)
The gravitational acceleration Log(g)	4.290(\pm 0.112)

may be broken and may evolve to be a broken-contact system as same as EP And (Liao et al. 2013).

Except for the long-term increase, there is also a cyclical change in Equation (2). Irwin (1952) proposed that light-time-travel effect (LTTE) from an additional body may lead to the periodic variation, and Applegate (1992) gave the other reason that the periodic variation may be due to magnetic activity cycles of one or both components. During recent years, much

Table 6
The Minimums Collected from the Literature

Min(HJD2400000+)	Type	Method	Ref.	Min(HJD2400000+)	Type	Method	Ref.
30938.4930	p	pg	(1)	51270.5095	p	ccd	(5)
30939.4030	s	pg	(1)	51274.5718	p	ccd	(5)
30941.4780	p	pg	(1)	51274.7560	s	ccd	(1)
30969.5120	p	pg	(1)	51280.8461	p	ccd	(6)
30972.4960	p	pg	(1)	51288.6060	p	ccd	(5)
30990.3770	s	pg	(1)	51306.8870	s	ccd	(6)
43347.4540	s	vis	(1)	51596.5835	p	vis	(1)
43358.3760	p	vis	(1)	51677.4556	p	ccd	(7)
43360.3800	s	vis	(1)	51684.4721	p	ccd	(8)
43387.3520	s	vis	(1)	51779.3752	p	ccd	(8)
43392.3650	p	vis	(1)	51956.6300	p	ccd	(8)
43394.3880	s	vis	(1)	52050.4270	p	ccd	(7)
43402.3410	p	vis	(1)	52105.4188	p	vis	(8)
43429.3020	p	vis	(1)	52105.4403	p	vis	(8)
43659.5350	s	vis	(1)	52105.4431	p	vis	(8)
43662.4890	s	vis	(1)	52105.4445	p	vis	(8)
43671.5350	p	vis	(1)	52116.5266	p	ccd	(7)
43674.4900	p	vis	(1)	52410.4754	p	ccd	(9)
43714.3930	p	vis	(1)	52489.5014	p	-Ir	(9)
43732.4680	p	vis	(1)	52492.4555	p	ccd	(8)
43746.3360	s	vis	(1)	52811.5060	p	ccd	(8)
44133.4830	p	vis	(1)	53075.9135	p	R	(10)
44142.3660	p	vis	(1)	53082.0075	s	ccd	(11)
44320.5480	s	vis	(1)	53121.8893	s	ccd	(11)
44458.4550	p	vis	(1)	53140.1528	p	V	(1)
44461.4040	p	vis	(1)	53517.3830	s	vis	(12)
45081.4230	p	pg	(2)	53601.3888	p	-Ir	(13)
46982.4610	p	vis	(1)	53855.8287	p	R	(14)
47691.4700	p	vis	(1)	53863.3991	s	-Ir	(13)
47691.4760	p	vis	(1)	53894.4196	s	-Ir	(13)
48444.4250	p	vis	(1)	53920.4549	p	-Ir	(13)
48444.4310	p	vis	(1)	53963.4725	s	-Ir	(15)
48444.4450	p	vis	(1)	54947.4145	p	-Ir	(16)
49512.4120	p	vis	(1)	54947.6009	s	-Ir	(16)
49885.5312	s	ccd	(1)	55640.5493	p	ccd	(17)
50585.4970	p	vis	(1)	55661.5985	p	-Ir	(17)
50641.6270	p	ccd	(1)	55670.4611	p	-Ir	(17)
50643.4751	p	ccd	(3)	56073.8983	s	V	(18)
51016.4443	p	ccd	(4)				

References. (1) <http://var2.astro.cz/ocgate/>; (2) Hoffmann 1983; (3) Safar & Zejda 2000a; (4) Safar & Zejda 2000b; (5) Safar & Miloslav 2002c; (6) Diethelm 2001; (7) Agerer & Hubscher 2002; (8) Braát et al. 2007; (9) Agerer & Hubscher 2003; (10) Dvorak 2005; (11) Nelson 2005; (12) Locher 2005; (13) Hubscher et al. 2006; (14) Nelson 2007; (15) Hubscher & Walter 2007; (16) Hubscher et al. 2010; (17) Hubscher et al. 2012; (18) Diethelm 2012.

research has pointed out that most contact binary stars exist in multiple systems (e.g., Pribulla & Rucinski 2006; D'Angelo et al. 2006; Liao & Qian 2010). We assuming the LTTE of third body is attributed to the periodic change of O-C. By using the following equation:

$$f(m) = \frac{(M_3 \sin i')^3}{(M_1 + M_2 + M_3)^2} = \frac{4\pi^2}{GT^2} \times (a'_{12} \sin i')^3, \quad (4)$$

we can obtain the mass function of the third body $f(m)$. In Equation (4), we use $a'_{12} \sin i' = A \times c$, where i' is the

inclination of the orbit of the third component, c is the speed of light, A is the amplitude of the LTTE, and a'_{12} is the semi-axis of the eclipsing-pair orbit around the common center of mass with the third body. The mass function is calculated to be $f(m) = 2.4 \times 10^{-4} M_{\odot}$. The mass of the additional body is tied up to its orbital inclination (i') and it cannot be counted as each one individually. When it is coplanar to the pair of binary system ($i' = 79.29$), its mass should be $M_3 = 0.098(\pm 0.029)$, and the orbital radius around the common center of mass is calculated to be

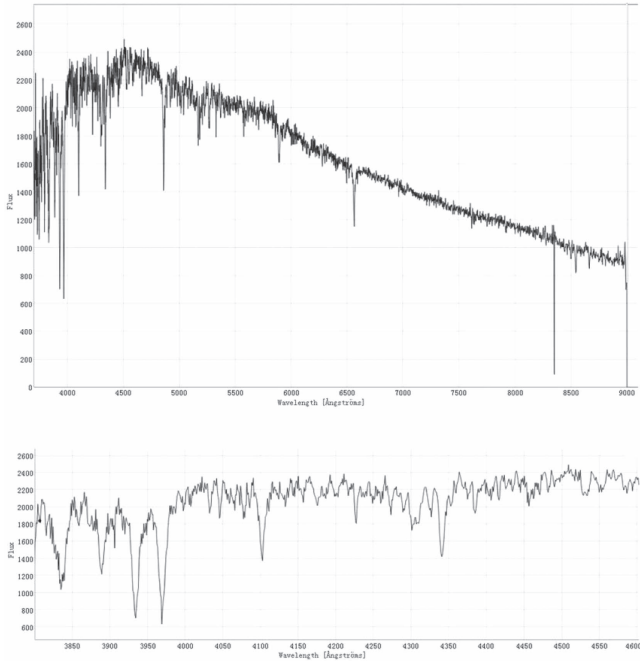


Figure 2. The spectrum of V502 Her from LAMOST.

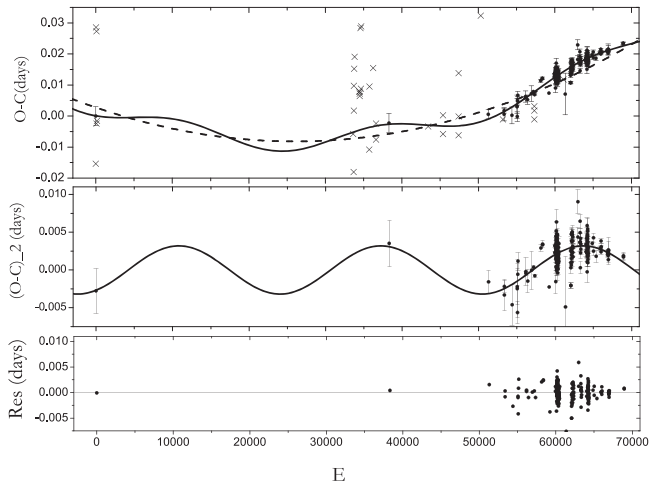


Figure 3. $O - C$ diagram of V502 Her calculated with the linear ephemeris of Equation (1) based on all available times of light minimum. The crosses refer to the visual and photographic observations, and the solid circles with error bar represent the photoelectric and CCD data in the upper panel. The middle panel is $(O - C)_2$ diagram of the photoelectric and CCD data by removing the quadratic ephemeris in Equation (2). The corresponding residuals are shown in the lower panel.

$a_3 = 10.6(\pm 4.3)$ AU. According the Cox (2000), it could be assumed to be a late M-type star, and it is difficult to detect the third body because of its extremely low luminosity. From

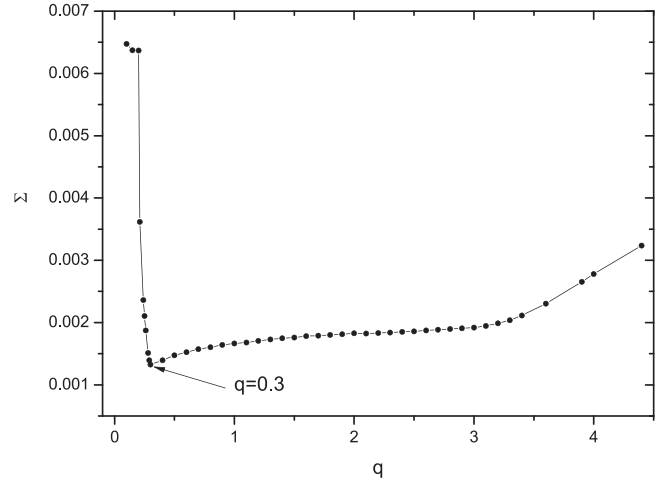


Figure 4. Relation between q and sum of residual for light curve of V502 Her. The lowest value for sum of residual is about $q = 0.3$

Table 7
Photometric Solutions for V502 Her

Parameters	Value	Errors
$g_1 = g_2$	0.32	Assumed
$A_1 = A_2$	0.5	Assumed
$T_1(K)$	6180	Assumed
Ω_{in}	2.4940	Assumed
Ω_{out}	2.2996	Assumed
$q(M_2/M_1)$	0.313	± 0.003
$T_2(K)$	6143	± 5
$i(^{\circ})$	79.29	± 0.15
$L_1/(L_1 + L_2)_B$	0.7265	± 0.0005
$L_1/(L_1 + L_2)_V$	0.7286	± 0.0005
$L_1/(L_1 + L_2)_R$	0.7295	± 0.0005
$L_1/(L_1 + L_2)_I$	0.7303	± 0.0005
$\Omega_1 = \Omega_2$	2.42	± 0.0009
$r_1/A(pole)$	0.4680	± 0.0007
$r_1/A(side)$	0.5070	± 0.0009
$r_1/A(back)$	0.5381	± 0.0009
$r_2/A(pole)$	0.2809	± 0.0003
$r_2/A(side)$	0.2951	± 0.0004
$r_2/A(back)$	0.3433	± 0.0009
$f(\%)$	38.1	± 2.9

Table 3, we find that there is different depth between phase 0.25 and 0.0 in different band. If the third body has low effective temperature, its radiation may be stronger in long wave than in short wave. During the solution of light curves, we also attempt to use the third light, but it cannot get the convergent solution and may also due to its low luminosity.

This work is partly supported by Chinese Natural Science Foundation (No. 11133007). We are indebted to the many observers who obtained the wealth of data on this eclipsing

Table 8
Some Contact Binary with the Increasing Period Change

Name	Period (days)	T_1 (k)	q	f (%)	dP/dt (10^{-7} days yr $^{-1}$)	Ref.
LO And	0.38043478	6500	0.371	30.5	+2.45	(1)
NO Cam	0.430754	6530	0.439	55.5	+5.34	(2)
V608 Cas	0.38040619	5660	0.373	19.1	+6.49	(3)
UZ Cmi	0.76195	6250	0.44	38.4	+0.41	(4)
AH Cnc	0.360477	6300	0.154	51.0	+4.29	(5)
V700 Cyg	0.34005	5770	0.5437	15.1	+0.28	(7)
V1191 Cyg	0.3133867	6215	0.107	68.6	+31.3	(6)
V502 Her	0.36927596	6180	0.313	38.4	+1.85	(8)
V868 Mon	0.637705	7400	0.373	58.9	+9.38	(9)

References. (1) Gürol & Müyesseröglü 2005; (2) Zhou et al. 2017; (3) Liu et al. 2016; (4) Qian et al. 2013; (5) Peng et al. 2016; (6) Ostadnezhad et al. 2014; (7) Yang & Dai 2009; (8) this paper; (9) Zhou et al. 2015.

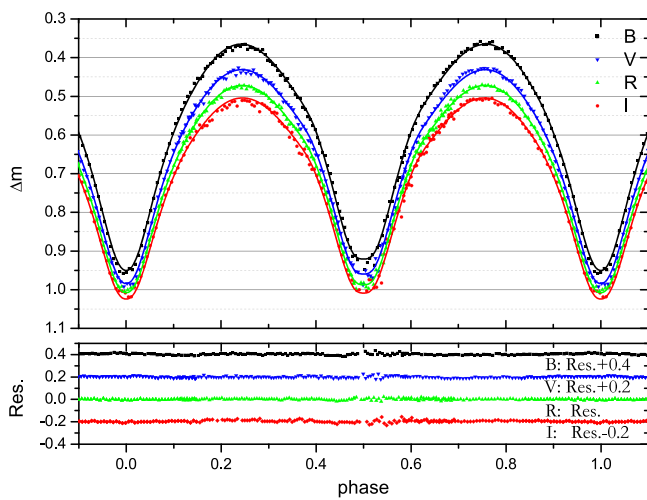


Figure 5. Theoretical light curve (solid lines) calculated by using the W-D method. The lower panel shows the residuals.

(A color version of this figure is available in the online journal.)

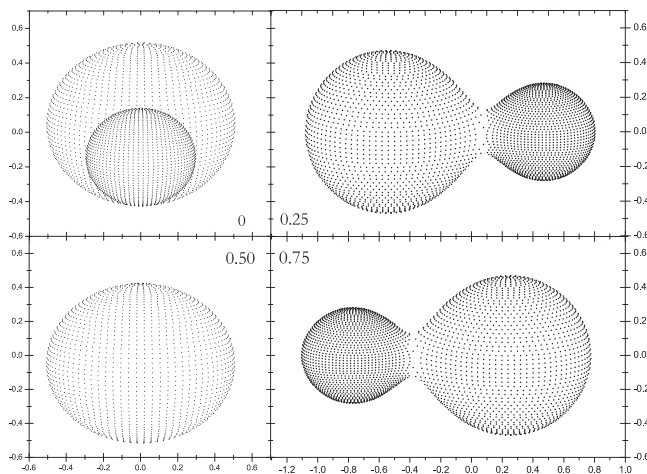


Figure 6. Geometrical structure of V502 Her at phases of 0.0, 0.25, 0.5, and 0.75, respectively.

binary system. We used the data observed with the 1-m, 60-cm telescope at Yunnan Observatories and 85-cm telescope at Xinglong Station of National Astronomical Observatories of China. This article also makes use of data from the DR1 of the WASP data (Butters et al. 2010) as provided by the WASP consortium, and the computing and storage facilities at the CERIT Scientific Cloud, reg. no. CZ.1.05/3.2.00/08.0144, which is operated by Masaryk University, Czech Republic.

References

- Agerer, F., & Hubscher, J. 2002, *IBVS*, **5296**, 1
Agerer, F., & Hubscher, J. 2003, *IBVS*, **5484**, 1
Applegate, J. H. 1992, *ApJ*, **385**, 621
Applegate, J. H., & Patterson, J. 1987, *ApJ*, **322**, 99
Brát, L., Zejda, M., & Svoboda, P. 2007, *OEJV*, **74**, 1
Butters, O. W., West, R. G., Anderson, D. R., et al. 2010, *A&A*, **520**, 10
Cox, A. N. (ed.) 2000, in *Allen's Astrophysical Quantities*, ed. A. N. Cox (4th ed.; New York: Springer)
D'Angelo, C., van Kerkwijk, M. H., & Rucinski, S. M. 2006, *AJ*, **132**, 650
Diethelm, R. 2001, *IBVS*, **5027**, 1
Diethelm, R. 2012, *IBVS*, **6029**, 1
Dvorak, S. W. 2005, *IBVS*, **5603**, 1
Flannery, B. P. 1976, *ApJ*, **205**, 317
Gazeas, K. D. 2009, *CoAst*, **159**, 129
Gessner, H. 1966, *Veroeff. Sternwarte Sonneberg.*, **7**, 61
Gray, R. O., & Corbally, C. J. 2009, *Stellar Spectral Classification* (Princeton, NJ: Princeton Univ. Press)
Gürol, B., & Müyesseröglü, Z. 2005, *AN*, **326**, 43
Hoffmann, M. 1983, *IBVS*, **2344**, 1
Hubscher, J., & Walter, F. 2007, *IBVS*, **5761**, 1
Hubscher, J., Lehmann, P. B., Moninger, G., Steinbach, H.-M., & Walter, F. 2010, *IBVS*, **5918**, 1
Hubscher, J., Lehmann, P. B., & Walter, F. 2012, *IBVS*, **6010**, 1
Hoffmann, M., & Meinunger, L. 1983, *IBVS*, **2343**, 1
Hoffmeister, C. 1949, *AnErg*, **12**, 1
Hubscher, J., Paschke, A., & Walter, F. 2006, *IBVS*, **5731**, 1
Irwin, J. B. 1952, *ApJ*, **116**, 211
Liao, W.-P., & Qian, S.-B. 2010, *MNRAS*, **405**, 1930
Liao, W.-P., Qian, S.-B., Li, K., et al. 2013, *AJ*, **146**, 79
Liu, L., Qian, S. B., He, J. J., et al. 2016, *NewA*, **43**, 1
Locher, K. 2005, *OEJV*, **3**, 1
Lucy, L. B. 1967, *ZA*, **65**, 89
Nelson, R. H. 2005, *IBVS*, **5602**, 1
Nelson, R. H. 2007, *IBVS*, **5760**, 1
Ostadnezhad, S., Delband, M., & Hasanazadeh, A. 2014, *NewA*, **31**, 14

- Peng, Y.-J., Luo, Z.-Q., Zhang, X.-B., et al. 2016, *RAA*, **16**, 157
Pribulla, T., & Rucinski, S. M. 2006, *AJ*, **131**, 2986
Qian, S. 2001, *MNRAS*, **328**, 914
Qian, S. 2003, *MNRAS*, **342**, 1260
Qian, S.-B., He, J. J., Zhang, J., et al. 2017, *RAA*, **17**, 87
Qian, S.-B., Li, K., Liao, W.-P., et al. 2013, *AJ*, **145**, 91
Robertson, J. A., & Eggleton, P. P. 1977, *MNRAS*, **179**, 359
Ruciński, S. M. 1969, *Acta Astron.*, **19**, 245
Safar, J., & Zejda, M. 2000a, *IBVS*, **4887**, 1
Safar, J., & Zejda, M. 2000b, *IBVS*, **4888**, 1
Safar, J., & Zejda, M. 2002c, *IBVS*, **5263**, 1
Van Hamme, W. 1993, *AJ*, **106**, 2096
Wilson, R. E. 1990, *ApJ*, **356**, 613
Wilson, R. E. 1994, *PASP*, **106**, 921
Wilson, R. E. 2012, *AJ*, **144**, 73
Wilson, R. E., & Devinney, E. J. 1971, *ApJ*, **166**, 605
Yang, Y.-G., & Dai, H.-F. 2009, *PASJ*, **61**, 57
Zhou, A.-Y., Jiang, X.-J., Zhang, Y.-P., & Wei, J. Y. 2009, *RAA*, **9**, 349
Zhou, X., Qian, S., He, J., Zhang, J., & Jiang, L. 2015, *PASJ*, **67**, 98
Zhou, X., Qian, S., & Zhang, B. 2017, *PASJ*, **69**, 37